

Cardiovascular, Pulmonary and Renal Pathology

# Circulating Angiogenic Precursors in Idiopathic Pulmonary Arterial Hypertension

Kewal Asosingh,<sup>\*†</sup> Micheala A. Aldred,<sup>‡§¶</sup>  
Amit Vasani,<sup>||</sup> Judith Drazba,<sup>||</sup> Jacqueline Sharp,<sup>\*†</sup>  
Carol Farver,<sup>\*||</sup> Suzy A.A. Comhair,<sup>\*†</sup> Weiling Xu,<sup>\*†</sup>  
Lauren Licina,<sup>\*†</sup> Lan Huang,<sup>\*\*</sup> Bela Anand-Apte,<sup>††</sup>  
Mervin C. Yoder,<sup>\*\*</sup> Rubin M. Tuder,<sup>‡‡</sup>  
and Serpil C. Erzurum<sup>\*†</sup>

From the Departments of Pathobiology,<sup>\*</sup> Pulmonary, Allergy, and Critical Care Medicine,<sup>†</sup> Genomic Medicine Institute,<sup>‡</sup> Imaging,<sup>||</sup> Lerner Research Institute, and the Cole Eye Institute,<sup>††</sup> The Cleveland Clinic, Cleveland, Ohio; the Taussig Cancer Center<sup>§</sup> and the Department of Genetics,<sup>¶</sup> Case Western Reserve University School of Medicine, Cleveland, Ohio; the Division of Cardiopulmonary Pathology,<sup>‡‡</sup> Johns Hopkins University School of Medicine, Baltimore, Maryland; and the Department of Pediatrics,<sup>\*\*</sup> Herman B. Wells Center for Pediatric Research, Indiana University School of Medicine, Indianapolis, Indiana

**Vascular remodeling in idiopathic pulmonary arterial hypertension (IPAH) involves hyperproliferative and apoptosis-resistant pulmonary artery endothelial cells. In this study, we evaluated the relative contribution of bone marrow-derived proangiogenic precursors and tissue-resident endothelial progenitors to vascular remodeling in IPAH. Levels of circulating CD34<sup>+</sup>CD133<sup>+</sup> bone marrow-derived proangiogenic precursors were higher in peripheral blood from IPAH patients than in healthy controls and correlated with pulmonary artery pressure, whereas levels of resident endothelial progenitors in IPAH pulmonary arteries were comparable to those of healthy controls. Colony-forming units of endothelial-like cells (CFU-ECs) derived from CD34<sup>+</sup>CD133<sup>+</sup> bone marrow precursors of IPAH patients secreted high levels of matrix metalloproteinase-2, had greater affinity for angiogenic tubes, and spontaneously formed disorganized cell clusters that increased in size in the presence of transforming growth factor- $\beta$  or bone morphogenetic protein-2. Subcutaneous injection of NOD SCID mice with IPAH CFU-ECs within Matrigel plugs, but not with control CFU-ECs, produced cell clusters in the Matrigel and proliferative lesions in surrounding murine tissues. Thus, mobilization of high levels of proliferative bone marrow-derived proangiogenic precursors is a characteristic of IPAH and may participate in the pul-**

**monary vascular remodeling process. (Am J Pathol 2008, 172:615–627; DOI: 10.2353/ajpath.2008.070705)**

Vascular remodeling of the small pulmonary arteries is a characteristic of pulmonary arterial hypertension (PAH) and results in the elevated pulmonary artery pressure and subsequently right heart failure and death. PAH may occur in association with other diseases and/or hypoxia, but in the absence of an associated disease, PAH is identified as idiopathic (IPAH).<sup>1</sup> IPAH is characterized pathologically by complex vascular lesions including neointima formation in small pulmonary arteries and plexiform lesions, which are comprised of disorganized monoclonal endothelial cell proliferation in a stroma of myofibroblasts.<sup>2,3</sup> Germline mutations in transforming growth factor (TGF)- $\beta$  receptor genes, primarily in the bone morphogenetic protein receptor 2 (*BMPR2*) gene, have been identified in the majority of patients with familial forms of IPAH<sup>4–8</sup> and in an average of 20% of individuals with sporadic IPAH.<sup>9–12</sup> On the basis of the known inhibitory effects of TGF- $\beta$  on endothelial and smooth muscle cell growth, it has been speculated that *BMPR2* mutations result in enhanced cell proliferation and pulmonary artery remodeling,<sup>13,14</sup> whereas the loss of BMP-dependent survival signals, and consequent endothelial cell apoptosis, have been proposed as an initiating step in some forms of experimental PAH<sup>15</sup> and in IPAH.<sup>16</sup> Thus, IPAH pathogenesis is generally proposed to result from an imbalance between pulmonary vascular cell proliferation and susceptibility to apoptosis. Recently, conclusive evidence that IPAH pulmonary artery endothelial cells (PAECs) have a hyperproliferative apoptosis-resistant phenotype as compared to cells from control lungs has been shown by means of cell proliferation, DNA synthesis, and evaluation of cell death pathways.<sup>17</sup> Ac-

Supported by the Cleveland Clinic Musculoskeletal Core Center (funded in part by the National Institute of Arthritis and Musculoskeletal and Skin Diseases Core Center grant no. 1P30 AR-050953) and the National Center for Research Resources (grants HL60917 and M01RR018390).

Accepted for publication November 29, 2007.

Address reprint requests to Serpil C. Erzurum, M.D., Lerner Research Institute, Cleveland Clinic, Department of Pathobiology, NC22, 9500 Euclid Ave., Cleveland, OH 44195. E-mail: erzurus@ccf.org.

cumulating evidence indicates that effector cells of lung disease originate from bone marrow-derived progenitors, revealing a previously unrecognized pathophysiological link between the bone marrow and the lungs.<sup>18–20</sup> Studies supporting this relationship are derived mainly from idiopathic pulmonary fibrosis in model systems, but recent studies also support a role for bone marrow-derived progenitors in remodeling of pulmonary arteries.<sup>21,22</sup>

The proliferation of endothelial cells and repair and/or remodeling of blood vessels is currently proposed to occur through complex interactions among mature endothelial cells within vessels and several different types of vascular stem cells, some of which are bone marrow-derived and others resident in the vessel. For example, growing numbers of reports indicate that a subset of bone marrow-derived progenitor cells in the peripheral blood circulation give rise to colonies of heterogeneous cells in culture including endothelial-like cells (colony-forming units of endothelial-like cells, CFU-ECs),<sup>23</sup> which play a key role in vascular health. Asahara and colleagues<sup>24</sup> first reported that CFU-ECs are enriched within the CD34<sup>+</sup> fraction of circulating mononuclear cells and that CFU-ECs are able to rescue mice from induced hind limb ischemia. In many reports,<sup>17,25,26</sup> cells that gave rise to CFU-ECs in culture were found to be particularly enriched within the CD34<sup>+</sup> and CD133<sup>+</sup> subsets, which led to the designation of the circulating subpopulation of CD34<sup>+</sup> CD133<sup>+</sup> cells as endothelial progenitor cells. Subsequent research has revealed that CD34<sup>+</sup> CD133<sup>+</sup> cells are bone marrow CD45<sup>+</sup> mononuclear cells, which are proangiogenic but not true endothelial cells.<sup>27</sup> Other studies<sup>28,29</sup> have identified that circulating CD14<sup>+</sup> monocytes are also capable of developing endothelial cell-like characteristics *in vitro*, and contribute to vascular homeostasis.<sup>28,30–32</sup> However, in contrast to CFU-ECs, the CD14<sup>+</sup> monocyte-derived endothelial-like cells do not form proliferative colonies *in vitro*. Studies have shown that CFU-ECs and CD14<sup>+</sup> monocytes, are involved in the genesis of vascular pathology.<sup>33–37</sup> Although the exact mechanisms of action are unknown,<sup>27</sup> there is growing evidence that CFU-ECs contribute to the formation of new blood vessels in a paracrine manner, possibly by disruption of mature endothelial cells lining the vessel walls or by interaction with high proliferative true endothelial progenitors, ie, the putative endothelial stem or colony-forming cell (ECFC), which serves as the actual building blocks of new vessels.<sup>27,38</sup> ECFCs are rare cells among mature endothelial cells and only a minor fraction, which may originate from the vascular wall endothelium, may be mobilized into the bloodstream and migrate through the blood circulation.<sup>27,39</sup> Specific cell markers that identify ECFCs are unknown, and hence a proliferative colony-forming cell assay is used to isolate these progenitors from circulation or from among endothelial cells in the vascular wall. The roles of these recently discovered ECFCs in vascular homeostasis and repair is in its infancy, but circulating ECFC numbers are increased in patients with coronary vascular disease.<sup>40</sup> Similarly, the interactions between ECFCs and CFU-ECs in the formation of new blood vessels are unknown. However, the relatively high frequency (400/ml blood) of CFU-ECs in

the circulation as compared to ECFCs (0.2/ml blood) suggests that CFU-ECs may arrive first at sites of injury and facilitate vascular repair by recruitment and activation of rare ECFCs,<sup>27</sup> and thus provide a trophic effect on neovascularization.<sup>32</sup> Here, we hypothesized that bone marrow-derived and/or tissue-resident endothelial progenitors may participate in the vascular remodeling of IPAH. To test this, circulating CD34<sup>+</sup>CD133<sup>+</sup> cells and CFU-ECs from individuals with IPAH or healthy controls, and resident endothelial progenitors (ECFCs) in the circulation and within IPAH and control pulmonary arteries were quantitated. CFU-ECs were further evaluated for their affinity toward mature endothelial cells *in vitro*, response to TGF- $\beta$ -family of cytokines, and proliferation *in vivo* by inoculation into immunocompromised mice.

## Materials and Methods

### Study Population

Individuals with known IPAH (class 1.1), familial form of PAH (class 1.2), and PAH secondary to sleep apnea or sarcoidosis (class 3.3 and 5.0) were enrolled in the study. Female nonsmoking volunteers with no known diseases and on no medications were recruited as the healthy control population. Venous blood was collected and processed within 6 hours of collection for evaluation of progenitor cells. Clinical information on all PAH volunteers, including pulmonary artery pressures from right heart catheterization, were available from medical history and records. The study was approved by the Institutional Review Board of the Cleveland Clinic, and written informed consent was obtained from all individuals.

### Mutation Analysis of *BMPR2*

Mutation analysis was performed on DNA extracted from peripheral blood leukocytes using the Qiagen DNA extraction kit (Qiagen Inc., Valencia, CA). The 13 exons of *BMPR2* and their flanking noncoding regions were amplified in 15 fragments by polymerase chain reaction (PCR) using the following standardized protocol. One times Hotstar mastermix was supplemented with 1 $\times$  Q solution (Qiagen), 0.2  $\mu$ mol/L primers (Table 1), and 20 to 30 ng of template DNA in a final volume of 10  $\mu$ l. Samples were subjected to 40 cycles of PCR, consisting of 30 seconds at 94°C, 30 seconds at 55°C, and 30 seconds at 72°C, with an initial incubation of 15 minutes at 94°C to activate the polymerase and a final extension of 10 minutes at 72°C. Half of the reaction was checked on a 1.5% agarose gel for specific amplification, and the remainder was used for sequencing. Excess primers and nucleotides were inactivated by treatment with shrimp alkaline phosphatase and exonuclease I. Samples were then cycle-sequenced using BigDye terminator chemistry (Applied Biosystems, Foster City, CA) and analyzed on a 3730xl capillary sequencer. Exon dosage analysis was conducted by multiplex ligation-dependent probe amplification using both a commercial kit (P093; MRC Holland,

**Table 1.** Primer Sequences for Amplification of BMPR2 Exons

Exon	Forward	Reverse
1	5'-CTGTATTGTGATACGGGCAGG-3'	5'-ATTAAGGCGGATTTCCCTGG-3'
2	5'-GGAAATTTATGAAGTCATTCGGA-3'	5'-GGATTTTAACTACTCCCATGTCC-3'
3	5'-TTGATTTGCAAACTGTTTCAT-3'	5'-TGCAAATCTTTGGAGAAAGGA-3'
4	5'-CTTTCTAAAGGGCAGTCTGTCA-3'	5'-TGGGTGATTTTGCATAACTTTG-3'
5	5'-GCTGCTAATCTTTCTGCAGCTC-3'	5'-TGAAGTCACTGTTCCAGGTCT-3'
6	5'-AGCAACAGAGAGCTGTAGCATT-3'	5'-TACAGGCATAAGCCACCACA-3'
7	5'-TTCCATCCCTTCTCCTCCT-3'	5'-CCTGTTGTGAATTTGAACCC-3'
8	5'-TTCATTTTCATGTTCAATAGTCCC-3'	5'-CACCTGGCCAGTAGATGTTTT-3'
9	5'-GGTTAATGACATGGTTAGGGTC-3'	5'-GCAATGAACTAAAGGTTTAAATGAA-3'
10	5'-TTGGTATCAGAAATACCCCTGTT-3'	5'-TTGTGGCATTAGGCAACTCC-3'
11	5'-GCATGTTCCGTAATCCTTGAA-3'	5'-TTCTTTGTTGGGTCTCAGTTTC-3'
12A	5'-TCAGAGGTGTTAAATTTGGAGAGAC-3'	5'-TCTGGGCCACTGAACTGTTT-3'
12B	5'-CAGCTGACAGAAGAAGACTTGG-3'	5'-ATATTGGGTTGTGGCAGCAT-3'
12C	5'-ATCAATGCAGCAGAACCTCAT-3'	5'-GCCCAAAGACACACAGG-3'
13	5'-TTGAGTTACATCCCTTACCCG-3'	5'-AAACATCTTCTGCATGTTTAAATGA-3'

Amsterdam, The Netherlands) and an in-house assay, as previously described.<sup>11</sup>

### Tissue Resident Endothelial Cells

IPAH and control PAECs were obtained from explanted IPAH human lungs and donor lungs not used in transplantation, respectively. The pulmonary arteries were finely dissected to the distal small arterioles, then cut longitudinally, and incubated with collagenase type II to detach endothelial cells. Cells were grown in MCB2-107 (Sigma, St. Louis, MO) on fibronectin-coated plates, and passaged at 70 to 80% confluence by dissociation from plates with 0.25% trypsin-ethylenediaminetetraacetic acid (Invitrogen, Carlsbad, CA). Primary cultures of passages 3 to 9 were used in experiments. The phenotype of endothelial cells was confirmed by immunocytochemistry for endothelial cell-type-specific markers (CD31, dilution 1/30; DAKO, Glostrup, Denmark, and von Willebrand factor, dilution 1/200; DAKO) and fluorescence-activated cell sorting (FACS) analyses for CD31 and VEGFR2 expression (Becton Dickinson, San Jose, CA). Immunohistochemical analysis of cultured cells identified that >95% were CD31-positive and >99% von Willebrand factor-positive. FACS analysis confirmed that >95% of the cells were CD31- and VEGFR2-positive. Human umbilical vein endothelial cells (HUVECs) were purchased from the American Type Culture Collection (Manassas, VA).

### ECFC Assays

ECFCs were quantified from PAECs obtained from explanted lungs or in the peripheral blood circulation of volunteers. Those obtained from the PAECs are referred to as vascular wall-resident ECFCs and those from the peripheral blood as circulating ECFCs. Frequency of these ECFCs was analyzed as described previously.<sup>41</sup> Briefly, single PAECs were sorted into collagen I-coated 96-well plates (one plate/sample) with EGM-2 medium (Cambrex, Walkersville, MD) supplemented with 20% fetal bovine serum. After 14 days of incubation the cell colonies were scored and frequency of high proliferative

ECFCs (colonies with >10,000 cells) were determined. For ECFCs in the blood circulation mononuclear cells were cultured on collagen I-coated six-well plates in EGM-2 medium plus 20% fetal bovine serum as described.<sup>41</sup> ECFCs were scored after 3 to 4 weeks.

### CFU-EC Assays

Colony formation CFU-ECs were assessed as described by Hill and colleagues,<sup>33</sup> by using the commercially available standardized form of this assay (CFU-EC Endocult Medium; Stem Cell Technologies, Vancouver, BC). Briefly, mononuclear cells were isolated from ethylenediaminetetraacetic acid blood by centrifugation on Ficoll-Paque Plus gradient (Amersham Biosciences, Piscataway, NJ), and a quantity of  $4.75 \times 10^6$  mononuclear cells were incubated in 1 ml of Endocult medium/well in fibronectin-coated 12-well plates (Becton Dickinson, Franklin Lakes, NJ). On day 2, nonadherent cells were harvested by gentle pipetting, counted, and seeded in fibronectin-coated 12-well plates at a density of  $1.9 \times 10^6$  cells/0.7 ml media. On day 5, wells were washed two times with warm EBM-2 media (Cambrex) to remove non-adherent and weakly attached cells. The number CFU-ECs/well was counted using an inverted microscope (Nikon, Tokyo, Japan) and were defined as a central core of round cells with more elongated spouting cells at the periphery. Number of cells/CFU-ECs in 20 random colonies was counted under a phase-contrast inverted microscope at a final magnification of  $\times 630$ .

### Clonality Analysis

DNA was extracted from total blood leukocytes and from CFU-EC cultures ( $1$  to  $3 \times 10^5$  cells) using Qiagen kits. X-inactivation patterns were determined using the HUMARA assay.<sup>42</sup> Briefly, this assay determines the methylation status of the human androgen receptor gene by combining analysis of a polymorphic trinucleotide repeat in exon 1 with restriction digestion of differentially methylated sites in the promoter, using methylation-sensitive restriction enzymes. Methylation

of the promoter marks the inactive X-chromosome in each cell. Analyses were conducted essentially as described<sup>42</sup> using *HhaI* as the methylation-sensitive enzyme and *RsaI* as the control enzyme. Samples were run on an ABI-3730xl sequencer (Applied Biosystems). Peak height ratios in *HhaI*-digested samples were normalized to control digests. Normalized ratios in CFU-ECs were then compared to total leukocyte DNA from the same patient.

### Flow Cytometry

CD34<sup>+</sup>CD133<sup>+</sup> bone marrow-derived proangiogenic progenitors in the peripheral blood circulation were quantified by staining with CD34-FITC (Becton Dickinson) and CD133-PE (Miltenyi Biotec, Auburn, CA) monoclonal antibodies. Isotype-matched irrelevant antibodies were used as negative controls for nonspecific binding. Samples were analyzed on a FACScan (Becton Dickinson) flow cytometer. Events ( $0.5 \times 10^6$ ) were acquired and data analysis is performed using Cell-Quest 3.3 software (Becton Dickinson). CFU-ECs were double-stained for CD34 and CD133 expression. In parallel, these cells were stained with CD31-FITC (Becton Dickinson), VE-Cadherin-PE (Becton Dickinson), CD14-FITC (eBiosciences, San Diego, CA), CD33-PE (eBiosciences), CD11b-biotin (eBiosciences), CD45-biotin (eBiosciences), and  $\alpha$ -smooth muscle actin-PE (R&D Systems, Minneapolis, MN). Streptavidin-PerCP (Becton Dickinson) was used a second step for biotinylated antibodies. Isotype irrelevant antibodies were used as negative controls for nonspecific binding. Samples were analyzed on a FACScan (Becton Dickinson) flow cytometer. At least 10,000 events were acquired and analyzed using Cell-Quest 3.3 software (Becton Dickinson).

### Gelatin Zymography

Equal volumes of supernatant/cell number were analyzed by gelatin zymography in a 7.5% polyacrylamide gel with 1 mg/ml of gelatin. After electrophoresis, gels were processed by washing with rinse buffer (50 mmol/L Tris, pH 7.5, 5 mmol/L CaCl<sub>2</sub>, 2.5% Triton) followed by incubation in buffer containing 50 mmol/L Tris, pH 7.5, 5 mmol/L CaCl<sub>2</sub> for 24 hours. Gels were rinsed and stained with Coomassie Blue for visualization of gelatinase activity.

### Affinity of CFU-ECs for *In Vitro* Angiogenic Tubes

Adhesion/incorporation of CFU-ECs to angiogenic tubes were assessed using the *In Vitro* Angiogenesis Assay (Chemicon International, Temecula, CA). CFU-ECs were harvested with trypsin and further cultured in EGM-2 medium (Cambrex) ( $0.7 \times 10^6$  cells/fibronectin-coated 24-well) for 1 to 2 weeks. Adherent CFU-ECs were harvested and fluorescently labeled with CellTracker Green (Molecular Probes, Eugene, OR). Tissue resident endothelial cells from different origins (HUVECs, IPAH PAECs, and control PAECs) were mixed with healthy control CFU-

ECs or IPAH CFU-ECs at a ratio of 9:1 in EGM-2 medium and seeded on the angiogenesis extracellular matrix in 24-well plates. After 8 hours, phase-contrast and fluorescence images of the endothelial cells in tube formation were acquired using a DM IRB inverted wide-field microscope (Leica, Heidelberg, Germany) with a  $\times 10$  objective and a MicroMax charge-coupled device camera (Photometrics, Tucson, AZ). The endothelial cells networks were manually delineated in the phase-contrast images of each field (three fields/sample) using Adobe Photoshop CS (San Jose, CA) and subsequently skeletonized using Image-Pro Plus 5.0 (Media Cybernetics, Silver Spring, MD). Total skeletal length and branch-to-branch lengths were extracted from the skeletonized images using Fovea 3.0 (Reindeer Graphics, Asheville, NC). To analyze CFU-EC adhesion/incorporation, binary image skeletons from phase-contrast images were used as masks for corresponding green-fluorescence images in Image-Pro Plus. The resulting green skeletons were thresholded to remove background fluorescence and green skeletal length was calculated using Image-Pro Plus. For each field, total green skeletal length was divided by the corresponding phase-contrast skeletal length to assess the contribution of CFU-ECs to the overall angiogenic tube formation (total green/total tube).

### Response of CFU-ECs to Cytokines of the TGF- $\beta$ Superfamily

Control or IPAH day-5 CFU-ECs were used to analyze their response to cytokines of the TGF- $\beta$  superfamily. Cells were harvested by trypsinization, washed, and resuspended in EBM-2 supplemented with 20% fetal calf serum. Either 1 ng/ml of TGF- $\beta$  (R&D Systems, McKinley Place, NE) or 100 ng/ml of BMP-2 (R&D Systems) was added to the medium. A quantity of  $0.7 \times 10^6$  cells/1 ml/24-well was seeded on solidified angiogenesis extracellular matrix. At day 9, the number of cell clusters/well were scored under an inverted microscope (Nikon). After fixation, specimens were stained with alcoholic eosin, washed, and mounted in Vectashield mounting medium with 4',6-diamidino-2-phenylindole (DAPI) (Vector Laboratories, Burlingame, CA). Images were collected using a TCS-SP AOBS confocal microscope (Leica Microsystems, Heidelberg, Germany) using a  $\times 20$ , 0.7 N.A. lens. The nuclei were visualized by exciting the specimen with the 351-nm line of an argon UV laser and collecting light from 400 to 480 nm. Cell clusters were visualized with 568-nm excitation from a krypton laser and emitted light collected from 575 to 700 nm. Confocal optical slices were collected with a 1- $\mu$ m step-size and the resulting z-series were reconstructed into a three-dimensional image using Volocity software (Improvision, Lexington, MA).

### *In Vivo* Inoculation of CFU-ECs

To analyze progenitor cell proliferation *in vivo*,  $1.2 \times 10^6$  day-5 CFU-ECs in EBM-2 medium with BMP-2 (100 ng/ml final concentration in 0.5 ml of Matrigel) was prechilled on ice and mixed with cold unpolymerized liquid Matrigel

(Becton Dickinson). Other growth factors were not incorporated into the Matrigel to avoid ingrowth of murine cells to the plug. This suspension was then slowly injected subcutaneously between the scapulae of immunodeficient NOD SCID (Jackson Laboratory, Bar Harbor, ME) mice using a cold syringe. At body temperature, the Matrigel quickly polymerizes to form a solid gel. After 4 weeks, animals were sacrificed and gels with surrounding tissues were removed and fixed in histochoice. Five- $\mu$ m sections were cut from paraffin-embedded samples and stained with hematoxylin/eosin or with anti-human  $\beta$ 2-microglobulin or Von Willebrand factor (DAKO) or  $\alpha$ -smooth muscle-actin (Abcam, Cambridge, MA) and histologically analyzed. For Von Willebrand factor, samples were pretreated with proteinase K for 8 minutes. Immunostaining was visualized by using diaminobenzidine and hydrogen peroxidase. All samples were stained by using an automated biotin-avidin-peroxidase system (Ventana-320-ES; Ventana Medical Systems, Tucson, AZ). Secondary antibody alone was used as negative control. All sections were counterstained with hematoxylin. Lesion sizes were quantified using Image-Pro Plus 5.0. Some  $\beta$ 2-microglobulin-stained slides were mounted in Vectashield mounting medium with DAPI (Vector Laboratories) and the nuclei were visualized using a Leica TCS-SP AOB confocal microscope (Leica Microsystems) using a  $\times$ 20, 0.7 N.A. lens. Specimens were excited with the 351-nm line of an argon UV laser and light was collected from 400 to 480 nm. Confocal optical slices were acquired with a 1- $\mu$ m step-size and the resulting z-series were reconstructed into a three-dimensional image using Volocity software (Improvision, Lexington, MA). The obtained images were analyzed by two independent individuals for quantification of percentage of human cell nuclei. For DNA fingerprinting, the Matrigel was microdissected from surrounding tissue on the

sections. Separated Matrigel and surrounding tissue were processed using the QIAamp DNA micro kit and amplified with four different microsatellite markers from chromosome region 2q37. Samples were analyzed on a 3730xl genetic analyzer (Applied Biosystems) and genotypes were compared to those obtained from leukocyte DNA of the same patient.

### Statistical Analysis

Data were analyzed by using JMP 5.1 software program. Analysis of variance or Student's *t*-test were used for comparisons of parametric data, and the Wilcoxon test was used for comparison of nonparametric data, as appropriate. *P* values <0.05 were considered as significant. Mean  $\pm$  SE value for each group is provided, unless indicated differently.

## Results

### Study Population

Peripheral venous blood was obtained from 16 IPAH patients, 3 of whom had the familial form of the disease (from two independent families), 4 patients with secondary pulmonary hypertension (Table 2), and 16 healthy female controls. Age, gender, and race were similar among healthy controls, IPAH [age (years): IPAH, 41  $\pm$  3; healthy controls, 38  $\pm$  3; *P* = 0.3; IPAH, one male/five African Americans; controls, no males/five African Americans; secondary pulmonary hypertension, 54  $\pm$  3, no males/two African Americans]. Medications were similar among patients, and included vasodilators and anticoagulants, and all patients were on supplemental oxygen (Table 2). In addition, explanted lungs were obtained at transplantation of five IPAH patients [age (years): 46  $\pm$  7;

**Table 2.** Population of Pulmonary Hypertension Patients

Patient	Venice classification	Age	Gender	Race	Associated disease	Vasodilator therapy
1	1.1	46	F	C	None	Bosentan, epoprostenol
2	1.1	39	F	C	None	Epoprostenol
3	1.1	33	F	C	None	Bosentan, epoprostenol, sildenafil
4	1.1	23	F	C	None	Bosentan, epoprostenol, sildenafil
5	1.1	55	F	C	None	Epoprostenol.
6	1.1	41	F	AA	None	Treprostinil
7	1.1	57	F	AA	None	Bosentan, esomeprazole, treprostinil
8	1.1	20	M	C	None	Epoprostenol
9	1.1	44	F	AA	None	Bosentan, epoprostenol, sildenafil
10	1.1	61	F	AA	None	Bosentan, epoprostenol
11	1.1	41	F	C	None	Epoprostenol
12	1.1	24	F	C	None	Bosentan, sildenafil
13	1.1	42	F	C	None	L-arginine, epoprostenol
14	1.2	53	F	C	None	Epoprostenol, sildenafil
15	1.2	29	F	C	None	Epoprostenol
16	1.2	56	F	C	None	Treprostinil
17	3.3	56	F	AA	Sleep apnea	Epoprostenol
18	3.3	52	F	C	Sleep apnea	Bosentan, epoprostenol
19	3.3	45	F	AA	Sleep apnea	Bosentan
20	5.0	63	F	AA	Sarcoidosis	Epoprostenol

C, Caucasian; AA, African American.  
 All patients were on supplemented oxygen.

two males/all Caucasians] and five donor lungs not used for transplantation as previously described.<sup>17</sup> Because of limitation of samples, all individuals were not evaluated in all experiments. The number of individual samples, and individuals evaluated, are noted in each experimental result.

BMPR2 mutation analysis was performed on all PAH participants and samples. A deletion of exon 3 was identified in two individuals with PAH from one family, which is predicted to result in deletion of 57 amino acid residues from the extracellular domain of the protein. No mutation was identified in the second familial PAH proband; however the combined techniques of sequence analysis and exon dosage measurements typically identify only ~70% of familial mutations.<sup>11</sup> Mutations were identified in two of the remaining IPAH cases (c.76 + 5G>A and c.296T>G, p.C99F); both are novel. Bioinformatic analysis of the G>A substitution at position 5 of the exon 1 splice donor signal using the MaxEntScan:score5ss program ([http://genes.mit.edu/burgelab/maxent/Xmaxentscan\\_scoreseq.html](http://genes.mit.edu/burgelab/maxent/Xmaxentscan_scoreseq.html)) gave a markedly lower maximum entropy score for the mutant sequence (3.53) than the wild-type (10.10). This mutation is therefore predicted to disrupt mRNA splicing, although RNA was not available from the patient to confirm this. The missense mutation C99F occurs at a conserved residue within the extracellular domain of BMPR2 and, although not reported previously, a different substitution (C99R) at the same position has been identified in both familial and IPAH cases.<sup>7</sup>

### Endothelial Progenitors and Proangiogenic Precursors

To evaluate whether there are high-proliferative ECFCs present within the pulmonary arterial wall of IPAH lungs, single cell analyses were performed on collagen I-coated 96-well plates, using PAECs derived from the pulmonary artery of normal donor lungs not used for transplantation, or explanted IPAH lungs. The numbers of vascular wall-resident ECFCs were similar among IPAH and control PAECs with one case of five control cultures and two cases of five IPAH PAEC cultures giving rise to high-proliferative ECFCs that formed colonies of >10,000 cells from the single cell that initiated the culture. In separate experiments, circulating ECFCs in the peripheral blood of IPAH patients was compared to healthy control volunteers. High-proliferative ECFCs were similarly detected in the circulating mononuclear cells of three of five IPAH patients and five of seven control volunteers. In contrast, early passage (passages 1 to 5) IPAH PAECs had significantly higher numbers of CD34<sup>+</sup> cells among the endothelial cells compared to control PAECs [%CD34<sup>+</sup> control 1.8 ± 0.7 (n = 4), IPAH 14.6 ± 1.9 (n = 4); P = 0.004].

Given the increased numbers of CD34<sup>+</sup> cells within cultures of IPAH PAECs, the presence of CD34<sup>+</sup>CD133<sup>+</sup> bone marrow-derived proangiogenic precursors in the peripheral blood was analyzed by FACS (Figure 1, A–F). A higher percentage of CD34<sup>+</sup>CD133<sup>+</sup> cells was present in the peripheral blood circulation of IPAH patients as compared with

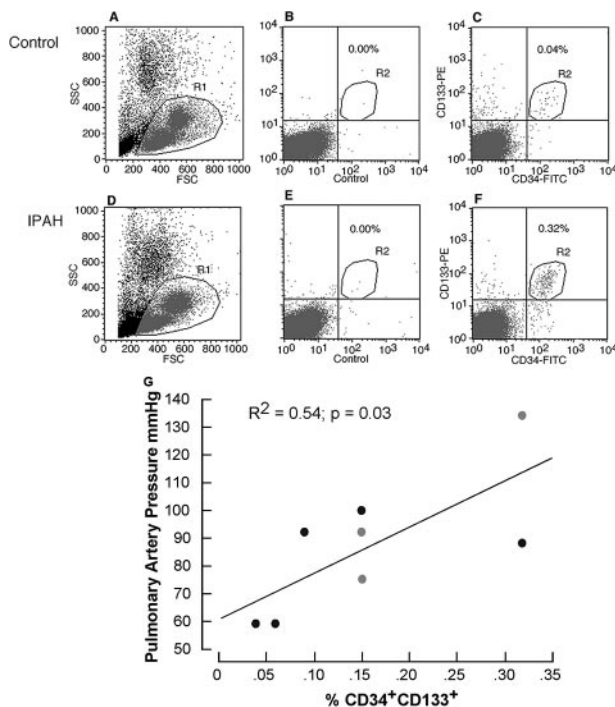


**Figure 1.** Circulating CD34<sup>+</sup> CD133<sup>+</sup> proangiogenic precursors in healthy control and IPAH patients. CD34<sup>+</sup> CD133<sup>+</sup> proangiogenic precursor cells in peripheral blood mononuclear cell fractions of healthy controls and IPAH patients were analyzed by FACS. **A** and **D**: Cell debris and remaining granulocytes were excluded by a lymphoblastoid gate (R1) on a forward scatter (FSC)/side scatter (SSC) dot plot. Quadrants were placed on FL1/FL2 dot plots based on negative control staining (**B**, **E**) and the cluster of CD34<sup>+</sup> CD133<sup>+</sup> cells defined within gate R2 (**C**, **F**). Noise/signal ratio (number of background events in R2/number of CD34<sup>+</sup> CD133<sup>+</sup> events in R2) of less than 0.05 was considered acceptable. **G**: Correlation between circulating CD34<sup>+</sup>CD133<sup>+</sup> progenitors and systolic pulmonary artery pressures. Familial patients are represented by gray symbols.

healthy controls [%CD34<sup>+</sup>CD133<sup>+</sup> cells: healthy control 0.051 ± 0.008 (n = 16), IPAH 0.15 ± 0.03 (n = 10), P = 0.006] (Figure 1G). Percentage CD34<sup>+</sup>CD133<sup>+</sup> cells in patients with pulmonary hypertension secondary to sleep apnea were similar to control levels (0.05 ± 0.02, n = 4). In IPAH the circulating CD34<sup>+</sup>CD133<sup>+</sup> cells were directly related to pulmonary arterial pressures (R<sup>2</sup> = 0.54, P = 0.03) (Figure 1B). IPAH patients had higher numbers of CFU-ECs derived from the circulating proangiogenic precursors compared with healthy controls [CFU-EC/24-well: healthy control 48 ± 7 (n = 7); IPAH 484 ± 83 (n = 11); P < 0.001] (Figure 2A). Numbers of CFU-ECs were related to percent CD133<sup>+</sup>CD34<sup>+</sup> cells (R<sup>2</sup> = 0.418, P = 0.005). These data identify that compared to healthy controls circulating CD34<sup>+</sup>CD133<sup>+</sup> proangiogenic precursors are increased in IPAH. Furthermore, CFU-ECs from IPAH patients had an approximately threefold higher number of cells per colony as compared with controls (cells/colony: healthy control, 27 ± 2; IPAH, 73 ± 2; P < 0.001). Frequency analysis revealed predominantly small colonies in healthy controls, whereas colonies were much larger in IPAH (Figure 2B).

To investigate whether the elevated numbers of circulating CD34<sup>+</sup>CD133<sup>+</sup> cells in IPAH represent a polyclonal expansion or the proliferation of a single aberrant clone, the pattern of X-inactivation was evaluated in CFU-EC cultures from five informative females by deter-

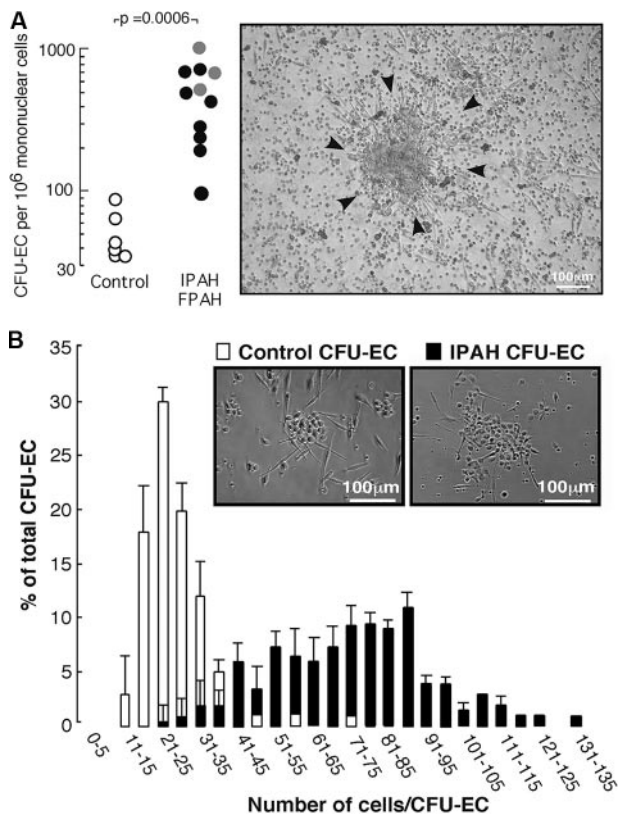


**Figure 2.** CFU-ECs in healthy controls and pulmonary hypertension patients. **A:** The number of CFU-ECs formed by CD34<sup>+</sup>CD133<sup>+</sup> progenitors from the blood mononuclear cell fractions. Image of a representative CFU-EC is shown. Logarithmic y axis. **B:** To measure proliferation, plates were washed and adherent cells in colonies were counted. IPAH CFU-ECs are larger compared to healthy control CFU-ECs (inset, phase contrast image of representative CFU-ECs of control and IPAH patient). Distribution of the CFU-EC colony size in terms of cell number/colony was analyzed as a parameter for the proliferation potential. CFU-ECs were grouped according to the indicated range of cell numbers/colony and their percentage in the total population of colonies calculated. Mean  $\pm$  SE values are shown.

mining the methylation status of the human androgen receptor gene promoter.<sup>42</sup> Approximately 1 to 3  $\times$  10<sup>5</sup> CFU-ECs were harvested and the X-inactivation pattern was compared to that in peripheral blood leukocytes from the same patient. In all five cases, the X-inactivation pattern of the CFU-ECs in culture did not differ from that observed in total peripheral blood leukocytes (not shown), indicating that the CFU-ECs consist of a polyclonal population.

### IPAH CFU-ECs Have Higher Affinity for Endothelial Cells and Form Large Cell Clusters in Response to TGF- $\beta$ and BMP2

Although the precise mechanisms by which CFU-ECs contribute to the vascular pathophysiology is currently unresolved, it is generally accepted that close interactions between CFU-ECs and endothelial cells are involved.<sup>43-45</sup> The *in vitro* endothelial cell tube formation assay, a model angiogenesis system, was used to evaluate the affinity of CFU-ECs for endothelial cells. Green-labeled CFU-ECs derived from IPAH or from healthy con-

trol patients were mixed with mature PAECs of control or IPAH patients or endothelial cells originated from umbilical cords (HUVECs). This mixture of CFU-ECs and mature endothelial cells was seeded on angiogenesis Matrigel and CFU-ECs associated to capillary tubes was analyzed. IPAH CFU-ECs associated with tubes formed by HUVECs, IPAH PAECs, and control PAECs. Normal CFU-ECs also adhered to the tubes, however this was significantly lower as compared to IPAH CFU-ECs (Figure 3, A and B). IPAH CFU-EC participation in tube formation was higher irrespective of the origin of mature endothelial cells (Figure 3B) ( $P = 0.0003$ ). However, control CFU-ECs had a tendency of greater affinity for angiogenic tubes with IPAH PAECs than control PAECs ( $P = 0.02$ ), suggesting an increased affinity of IPAH PAECs for CFU-ECs.

Because of the known abnormalities in TGF- $\beta$  family receptor signaling in IPAH,<sup>46</sup> even in the absence of BMP2 mutations, the response of CFU-EC-derived cells to cytokines of this family was evaluated. CFU-ECs were incubated in an angiogenic Matrigel in the presence of TGF- $\beta$ , BMP-2, or media alone (Figure 3C). IPAH CFU-ECs formed three-dimensional cell clusters in Matrigel with media alone, in contrast to control CFU-ECs (Figure 3D). In the presence of TGF- $\beta$ , the number of cell clusters in IPAH increased and BMP-2 induced a maximum number of these structures. Control CFU-ECs exhibited a low-level response of cell cluster formation to cytokines, with lesser numbers and visibly smaller clusters than with IPAH cells. These results not only indicate that IPAH CFU-ECs have a higher affinity for endothelial cells, but also that IPAH PAECs have a higher affinity for CFU-ECs. In addition, IPAH CFU-ECs exhibit aberrant response to TGF- $\beta$  and BMP-2, two cytokines with crucial roles in IPAH.

### MMP Production by CFU-ECs

To evaluate the proangiogenic environment that is created by CFU-ECs, supernatants collected from CFU-ECs after overnight incubation in serum-free medium (EBM-2) were used to analyze secreted matrix metalloproteinase (MMP)-9 and MMP-2. MMP-9 and MMP-2 activity were detected in supernatants from IPAH and control CFU-ECs (Figure 4). There was no difference in MMP-9 secretion, but CFU-ECs derived from IPAH patients produced significantly higher levels of MMP-2. Thus, CFU-ECs in IPAH patients are increased in the circulation and are functionally different in proangiogenic potential. These cells form larger colonies, have an enhanced affinity for endothelial cells, form abnormal cell clusters, in particular in response to BMP-2, and secrete high levels MMP-2.

### IPAH CFU-ECs Are Invasive and Form Angioproliferative Lesions *in Vivo*

These results prompted us to analyze the growth of these cells *in vivo*. For this purpose, IPAH or control CFU-ECs, were suspended in Matrigel containing BMP-2 and subcutaneously engrafted into NOD SCID mice. After 4

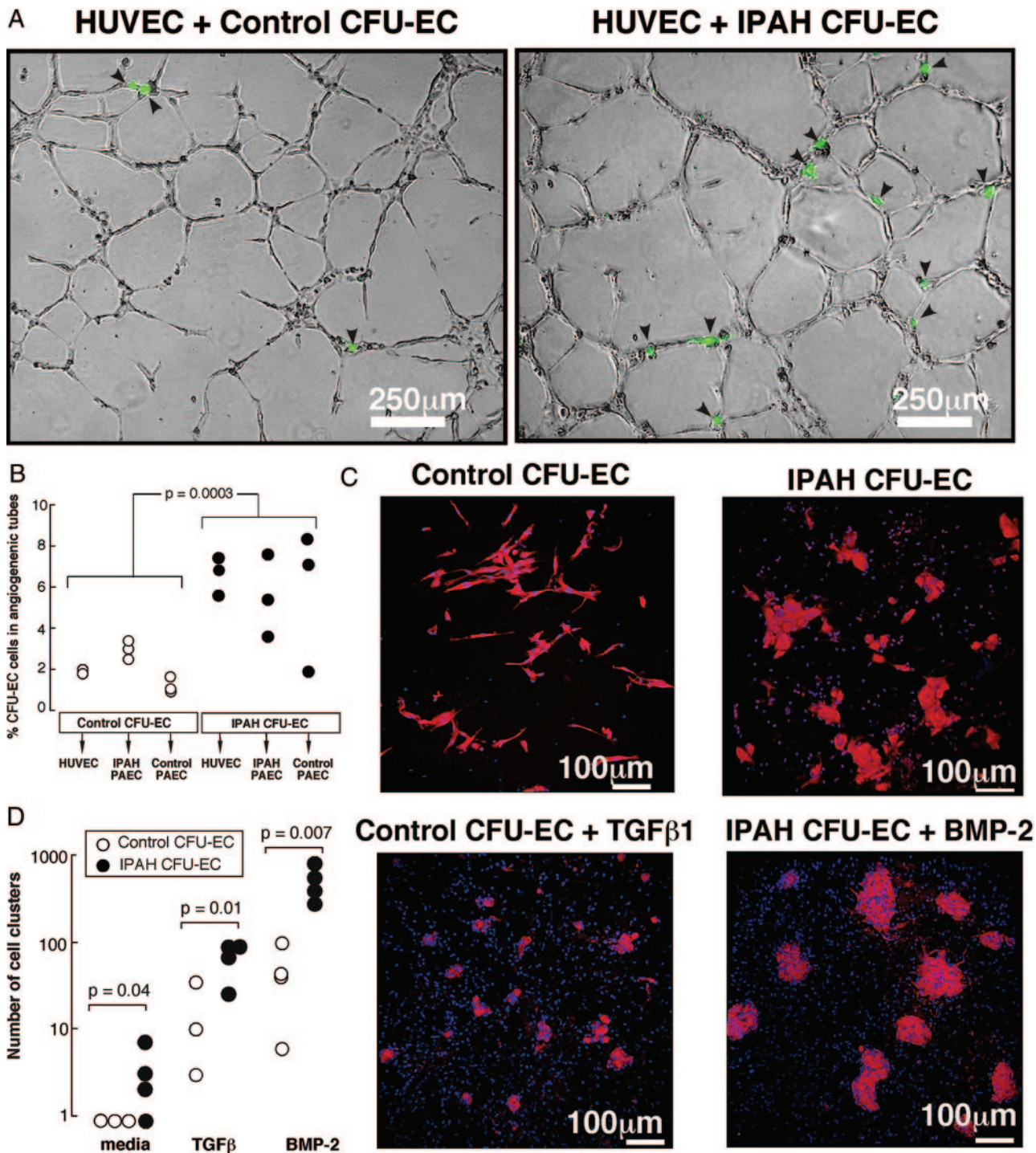


**Figure 3.** Affinity of CFU-ECs for PAECs and formation of cell clusters. **A:** The affinity of CFU-ECs for tubes formed by endothelial cells was analyzed in an *in vitro* angiogenic assay. Green fluorescent labeled CFU-ECs and nonlabeled PAECs (PAECs) from different origins were mixed and seeded on angiogenesis extracellular matrix. After 8 hours, a network of angiogenic tubes were formed and associated CFU-ECs were analyzed. Angiogenic tube formation by HUVECs in the presence of control CFU-ECs (**left**) and by HUVECs in the presence of IPAH CFU-ECs (**right**). **Arrows** indicate green associated CFU-ECs. **B:** Quantitation of CFU-ECs associated to tubes formed by endothelial cells (HUVECs, IPAH PAECs, and control PAECs). Each **dot** represents a value from a single IPAH patient (**filled dots**) or healthy control subject (**open dots**). **C:** To analyze responses of control and IPAH CFU-ECs alone, cells were cultured on angiogenic extracellular matrix in the presence of TGF- $\beta$ , BMP2, or medium alone. Confocal microscopy imaging of the cells in different conditions is illustrated. **Top:** Clear morphological difference between control and IPAH CFU-ECs under basal conditions. **Bottom:** Cell clustering in the presence of TGF- $\beta$  or BMP2. Control and IPAH CFU-ECs have distinct cell clustering morphology and representative pictures of the types of clusters are shown. IPAH CFU-ECs formed the largest cell clusters. **D:** IPAH CFU-ECs formed cell clusters even in the absence of TGF- $\beta$  or BMP2. Number of cell clusters was greatest in IPAH CFU-ECs grown in the presence of BMP2. Each **dot** represents a value from a single patient (**filled dots**) or healthy control subject (**open dots**). Cells used in these experiments did not have BMP2 mutations.

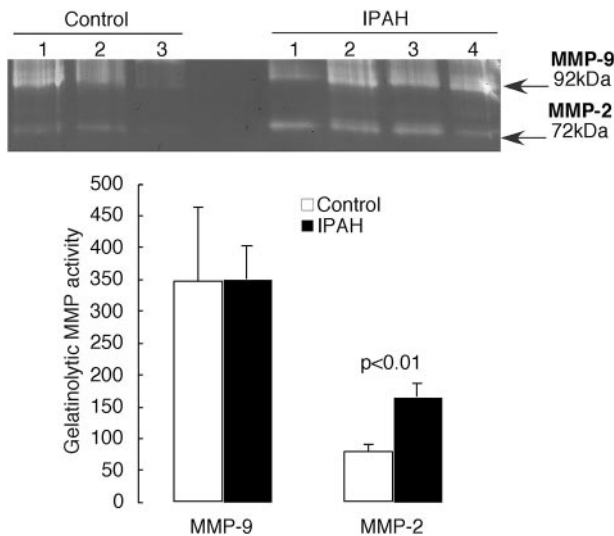


**Figure 4.** MMP activity of CFU-ECs. MMP activity in serum-free media overlying CFU-ECs was measured by gelatin zymography. Zymograph of three control CFU-ECs and four IPAH CFU-ECs are shown. Activity was quantified by densitometry. Equal volume of supernatant/cell was loaded per lane. Mean ± SEM values are shown.

weeks, the Matrigel plugs and surrounding tissues were removed and analyzed. Figure 5 shows the phenotype of the CFU-ECs before injection. IPAH and control CFU-ECs had a similar phenotypic cellular composition of

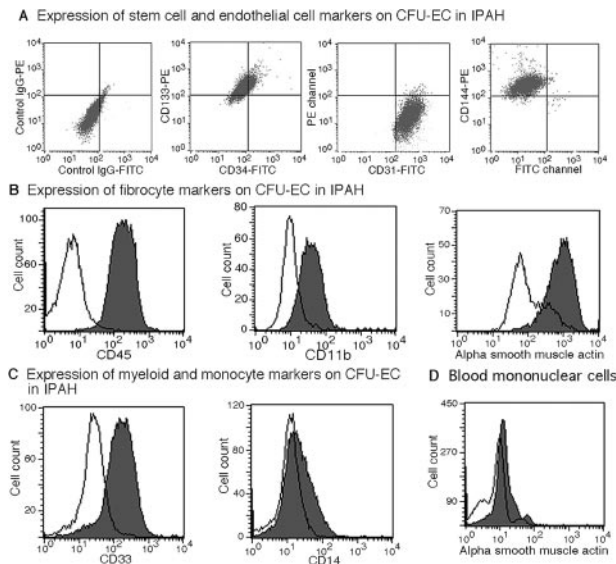


**Figure 5.** Phenotypic profile of CFU-ECs. **A:** CFU-ECs expressed stem cell markers CD34 and CD133 and endothelial cell markers CD31 and VE-cadherin. Representative dot plots from FACS analyses of IPAH-derived CFU-ECs are shown. **B:** In addition to the stem cell and endothelial cell markers in **A**, the cells also expressed CD45, CD11b, and  $\alpha$ -smooth muscle actin, markers of fibrocyte lineage. Open histograms indicate background staining with isotype-matched negative control antibodies. Histograms (shaded) from representative IPAH-derived CFU-ECs are shown. **C:** Analyses of CFU-ECs for expression of myeloid marker CD33 and monocyte marker CD14. Open histograms indicate background level staining with isotype-matched negative control antibodies. Histograms (shaded) from representative IPAH-derived CFU-ECs show high-level CD33 expression, but not CD14. **D:** Peripheral blood mononuclear cells stained as negative control for the  $\alpha$ -smooth muscle actin antibody. Open histogram indicates background level staining with isotype-matched negative control antibodies. Histogram (shaded) of cells from one representative patient, reveal no significant expression of this fibrocyte marker in freshly obtained circulating mononuclear cells.

CD133<sup>+</sup>CD34<sup>dim</sup>CD31<sup>+</sup>CD144<sup>+</sup>CD45<sup>+</sup>CD11b<sup>+</sup>SMA<sup>+</sup>CD33<sup>+</sup>CD14<sup>-</sup>. After inoculation into NOD SCID mice, IPAH-derived CFU-ECs formed cell clusters in the Matrigel plug whereas control CFU-ECs formed no detectable cell clusters (Figure 6, A–F). In addition to the cell clusters within the Matrigel plug, IPAH cells demonstrated human cell lesions outside the Matrigel plug, with extension within the subcutaneous tissues of the mouse (Figure 6, B and G–P). Staining with human-specific  $\beta$ 2-microglobulin antibodies confirmed that the cells in cell clusters and angioproliferative lesions were of human origin (Figure 6, E, H, K, L, Q, and P). In two experimental animals, IPAH CFU-EC-derived cells infiltrated surrounding tissue structures of nerve and skeletal muscle (Figure 6, G, H, O, and P). The relative numbers of human and mouse cells were further confirmed by confocal microscopy analysis of nuclear organization, and DNA fingerprinting using microsatellite analysis. Mouse and human cell nuclei each have unique structural organization observable by DAPI staining pattern, allowing discrimination and quantitation of human and mouse cells. Cells within the Matrigel plug were uniformly human, whereas cells within lesions outside the plug consisted of 90.5 ± 3.5% human cells (Figure 7A). Furthermore, the genotypes obtained from cells within the plug and from cells invading outside the plug matched that of leukocyte DNA of the same patient, confirming that these clusters are human cells derived from the injected CFU-ECs (Figure 7B).

## Discussion

Nearly 3 decades ago, Smith and Heath<sup>47</sup> postulated that vasoformative cells arriving from the blood stream contribute to the formation of plexiform lesions. Here, we provide evidence that the vascular remodeling occurring in the lungs of patients with IPAH is associated with elevated numbers of circulating CD34<sup>+</sup>CD133<sup>+</sup> proangiogenic precursors. Furthermore, these bone marrow-derived progenitors are shown to give rise to increased numbers of proliferative CFU-ECs that are enriched in CD34 and CD133 fractions.<sup>17,24–26</sup> The conclusive evidence that CFU-ECs are bone marrow-derived<sup>27</sup> makes it unlikely that these cells originate from the diseased lung, but the diseased lung vascular microenvironment may promote the mobilization of these proangiogenic cells from the bone marrow and their subsequent recruitment into lung vessels. It may also be possible that the changes in the bone marrow-derived cells may be related to the medications used in this condition, neurohormonal or hemodynamic effects of PAH, or to an enhanced inflammatory state.<sup>48,49</sup> T cells are present in the inflammation associated with IPAH vascular lesions<sup>48</sup> and T-cell-mediated inflammation is critical for neovascularization in hind limb ischemia models,<sup>23,50,51</sup> in the allergen challenge murine model of asthma,<sup>20</sup> and plays an important role in CFU-EC formation.<sup>23</sup>

Our group recently reported that IPAH PAECs have an apoptosis-resistant and hyperproliferative phenotype in cell culture.<sup>17</sup> Although high-proliferative vascular wall-derived progenitors were not increased in IPAH endothe-

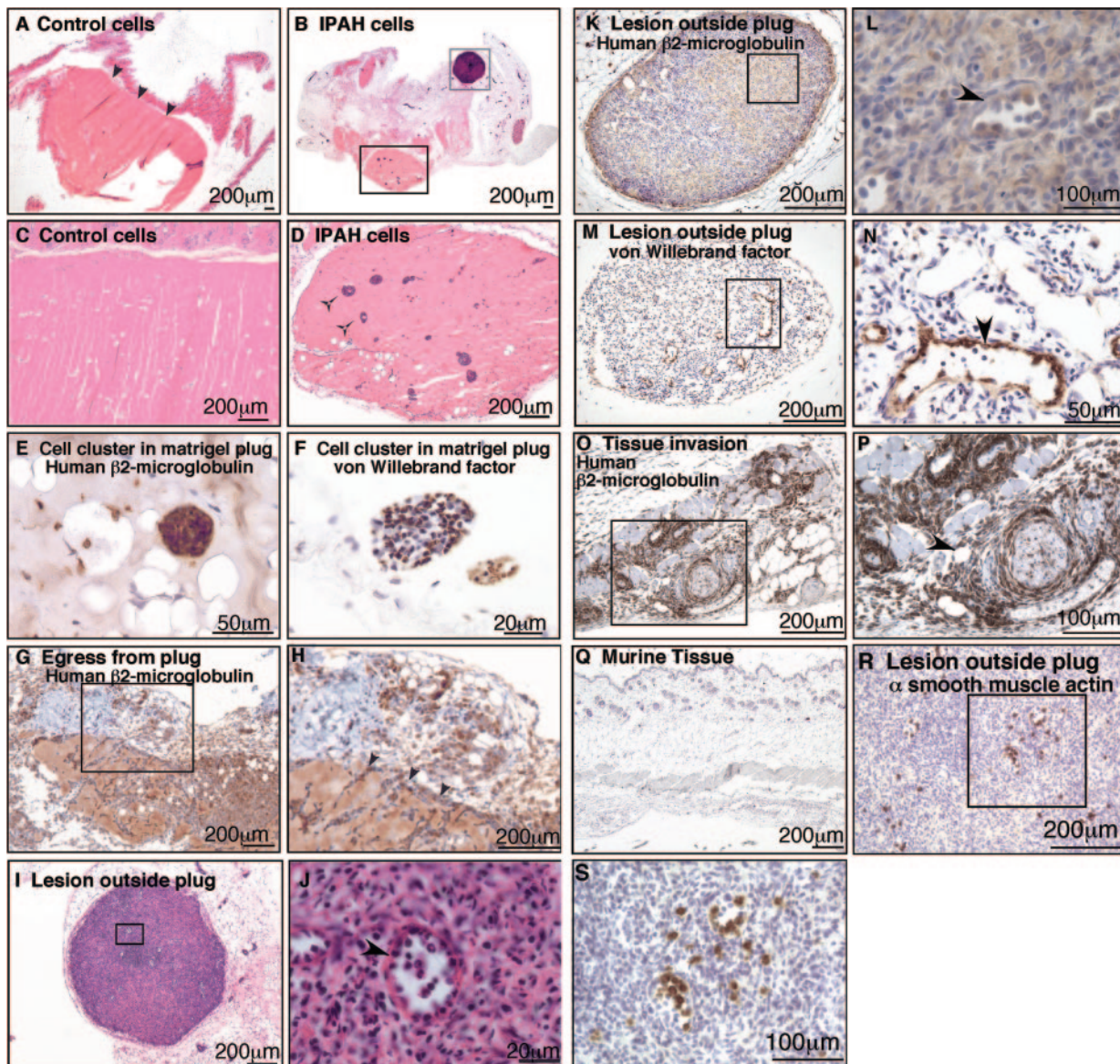


**Figure 6.** Histology of murine tissues and human cells 4 weeks after inoculation of NOD SCID mice with CFU-ECs derived from controls (**A, C**) or IPAH patients (**B, D–R**) within Matrigel plugs. **A** and **C**: Healthy control CFU-EC-EC injection. Matrigel plug (**arrowheads**) with overlying murine skin, with no evident cell clusters. High power of Matrigel region indicated in **A** is shown in **C**. **B** and **D**: Murine subcutaneous tissue containing Matrigel plug with cell clusters from IPAH-CFU-ECs (**lower boxed area**) and a lesion distant to the plug (**upper boxed area**). High power of **lower box region** from **B** is shown in **D**, with **arrows** identifying two cell clusters with central lumens. **E**: Cell cluster is identified as containing human cells by positivity for human  $\beta 2$ -microglobulin. **F**: Cells within the Matrigel plug have immunoreactivity to human von Willebrand factor indicating endothelial cell-like differentiation. **G** and **H**: Identification of human cells within and outside of Matrigel plug by  $\beta 2$ -microglobulin positivity. IPAH-derived cells egress from the plug into the adjacent mouse tissue. High power **H** is region of **boxed area** in **G**. **Arrows** in **H** delineate the plug and mouse tissue interface. **I** and **J**: Human cell lesion within murine subcutaneous fat tissue containing multiple vascular structures. **J**: High-power view of the **boxed region** in **I** with vascular structures (**arrow**). **K** and **L**: Cells in lesion are identified as human by positivity for human  $\beta 2$ -microglobulin. **L**: Higher magnification of **boxed region** from **K** shows variable intensity but all cells positive for  $\beta 2$ -microglobulin. Vessel lumen indicated by **arrow**. **M** and **N**: Identification of endothelial cells in the lesion by von Willebrand factor staining. **N**: Lesions outside the Matrigel plug were variably immunoreactive for von Willebrand factor but vessel-like structures within lesions were strongly immunoreactive (**arrow**). **Boxed area** in **M** rotated 90° counter clock-wise shown at high power in **N**. **O** and **P**: Human cells that are  $\beta 2$ -microglobulin-positive infiltrate the skeletal muscle and adjacent nerve in mouse subcutaneous tissue. **P**: Higher magnification of **box region** of **O** shows immunoreactive human cells around nerve and muscle (**arrow**). **Q**: Immunostaining with human  $\beta 2$ -microglobulin shows no cross-reactivity with murine subcutaneous tissues. **R** and **S**: Lesions outside the Matrigel plug contain  $\alpha$ -smooth muscle actin-positive cells, primarily found in association with vessel-like structures. High-power view of the **boxed region** in **Q**.

lial cell cultures in the present study, the expansion of endothelial cells is driven by proliferation of both high-proliferative and low-proliferative vascular progenitors, the latter of which were not quantified in the current study. Conversely, IPAH PAEC cultures contained greater than normal numbers of CD34<sup>+</sup> cells, which suggests a role for these cells in the more rapid growth of IPAH endothe-

lial cells in culture. In fact, the *in vitro* and *in vivo* assays in the present study document that CFU-ECs from IPAH patients have a significant enhanced angioproliferative potential. In support of a possible intrinsic alteration of these bone marrow-derived cells, IPAH CFU-ECs form disorganized clusters in response to cytokines of the TGF- $\beta$  superfamily, in particular BMP-2. Greater affinity of

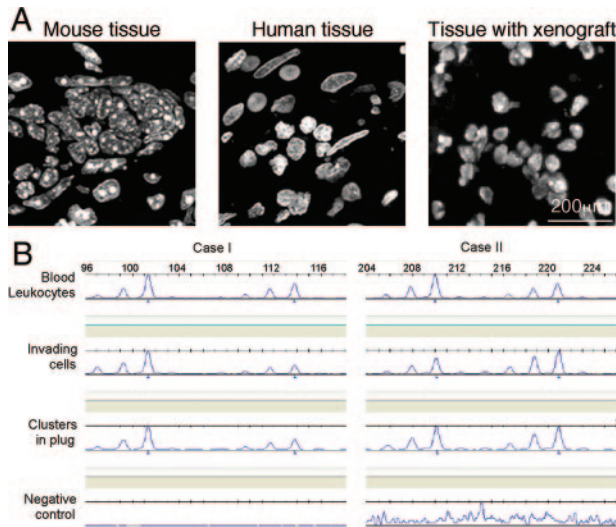


**Figure 7.** DAPI staining of nuclei and microsatellite analysis of cells xenografted into NOD SCID mice. **A:** Nuclei of cells inside the Matrigel plug and outside the plug were analyzed for DAPI staining pattern. Mouse and human cells have distinctive DAPI staining of the nucleus. Nuclei of xenografted tissue mainly consist of human cells. **B:** Microsatellite genotyping was used to definitively confirm that the origin of the cells inside the Matrigel plug and the invading cells in the surrounding tissue were patient derived.

IPAH CFU-ECs to angiogenic tubes compared to control CFU-ECs also supports intrinsic alterations of these cells in IPAH. Furthermore, the trend of a greater adhesion of control CFU-ECs to IPAH-derived pulmonary endothelial cells than to normal endothelial cells raises the possibility that an increased affinity or an active recruitment of CFU-ECs by IPAH pulmonary arterial endothelial cells may also occur. Once recruited, the release of matrix metalloproteinases by CFU-ECs as shown in this study, and other factors reported by others,<sup>52</sup> may foster an angiogenesis response in the pulmonary artery. Specifically, IPAH CFU-ECs produced much more MMP-2, a protease that plays crucial roles in vascular regeneration. MMP-2-deficient mice are severely impaired in their angiogenesis response to ischemia attributable to impaired proliferative and mobilization/invasive responses of hematopoietic progenitor-derived angiogenic precursors.<sup>53</sup> The impairment in angiogenesis is restored by transplantation of bone marrow-derived mononuclear cells from MMP-2<sup>+/+</sup> mice.<sup>53</sup> Previous reports indicate that bone marrow-derived proangiogenic progenitors trigger neovascularization through disruption of pre-existing blood vessels.<sup>54,55</sup> Thus, CFU-ECs may play an active role in the promotion of proliferative vascular lesions in IPAH by disruption and activation of the endothelium through release of matrix metalloproteinases and other angiogenic factors. However, the ability of bone marrow cells to mimic blood vessels also raises the possibility that CFU-ECs may incorporate into vessels through a process of vasculogenic mimicry<sup>56</sup> and contribute directly to the formation of plexiform lesions.

Although this study does not address directly whether the CFU-EC population participates in the genesis of IPAH, we modeled the local growth with *in vivo* inoculation of the IPAH CFU-ECs into the immune-deficient SCID mice, a reliable approach used to evaluate dysregulated

cell proliferation. In contrast to healthy controls, IPAH CFU-ECs formed large clusters and invasive angioproliferative lesions extrinsic to the Matrigel plug, which confirmed that bone marrow-derived cells with a heightened growth potential are mobilized in IPAH. One explanation for more proliferative precursors in IPAH may be that more primitive progenitors are mobilized into the circulation, which have a survival/growth advantage especially in the hypoxic milieu of the Matrigel plug. In this context, the mobilization of proangiogenic bone marrow-derived cells may be a normal physiological repair response to ongoing pulmonary vascular shear stress and endothelial injury. In support of this, progenitor cell mobilization is intrinsic to hypoxic conditions,<sup>57</sup> and increased bone marrow progenitors have been reported in hypoxia-induced animal models of PAH.<sup>58,59</sup> However, even if the greater number of circulating cells is part of a reparative response, the aberrant response to TGF- $\beta$  and BMP-2 *in vitro*, release of high amounts of MMP-2 and the invasive nature of the CFU-ECs in the xenograft model, strengthen the hypothesis that proangiogenic bone marrow-derived cells might contribute to the progression of IPAH. The associative observations of IPAH together with bone marrow-related hematological disorders supports the concept that bone marrow-derived cells may be the link between the occurrences of these processes. For example, in proliferative disorders of the hematopoietic stem cell, such as myeloproliferative cancers, there is a relatively high unexplained incidence of IPAH,<sup>60–62</sup> and radiation therapy or chemotherapy has been reported to result in improvement or regression<sup>63,64</sup> of IPAH. Regardless of the role bone marrow-derived precursors play in the disease process, mobilization of these cells is a characteristic of IPAH patients, which offers an opportunity for mechanistic studies using human circulating cells as opposed to lung vascular tissues. These findings also provide a novel noninvasive approach for the systematic investigation of pulmonary vascular remodeling through the evaluation of CD34<sup>+</sup>CD133<sup>+</sup> cells and CFU-ECs as biomarkers. In contrast, the circulating CD14<sup>+</sup> monocyte cells from IPAH patients<sup>16</sup> do not form proliferative lesions when inoculated into NOD SCID mice (data not shown), confirming that these cells, which are being used in human clinical trials, are unlikely to contribute to hyperplastic endothelial lesions. Future studies are required to determine how the bone marrow-derived proangiogenic precursors and pulmonary vascular wall endothelial resident progenitors interact in IPAH, and if novel therapeutic approaches that target nonproliferative angiogenic mononuclear cells<sup>65</sup> will impact on the remodeling and outcomes of IPAH.

### Acknowledgments

We thank D. Laskowski and M. Baakli for assistance with volunteer recruitment; P. Harbor and the Lerner Research Institute Genomics Core for sequencing/genotyping support; A. Arroliga, R. Dweik, and C. Jennings for helpful discussions; and David Schumick, B.S., C.M.I.,

Cleveland Clinic Center for Medical Art and Photography for illustrations.

## References

1. Simonneau G, Galie N, Rubin LJ, Langleben D, Seeger W, Domenighetti G, Gibbs S, Lebec D, Speich R, Beghetti M, Rich S, Fishman A: Clinical classification of pulmonary hypertension. *J Am Coll Cardiol* 2004, 43:5S–12S
2. Cool CD, Stewart JS, Werahera P, Miller GJ, Williams RL, Voelkel NF, Tuder RM: Three-dimensional reconstruction of pulmonary arteries in plexiform pulmonary hypertension using cell-specific markers. Evidence for a dynamic and heterogeneous process of pulmonary endothelial cell growth. *Am J Pathol* 1999, 155:411–419
3. Voelkel NF, Tuder RM: Severe pulmonary hypertensive diseases: a perspective. *Eur Respir J* 1999, 14:1246–1250
4. Lane KB, Machado RD, Pauciulo MW, Thomson JR, Phillips III JA, Loyd JE, Nichols WC, Trembath RC: Heterozygous germline mutations in BMPR2, encoding a TGF-beta receptor, cause familial primary pulmonary hypertension. The International PPH Consortium. *Nat Genet* 2000, 26:81–84
5. Deng Z, Morse JH, Slager SL, Cuervo N, Moore KJ, Venetos G, Kalachikov S, Cayanis E, Fischer SG, Barst RJ, Hodge SE, Knowles JA: Familial primary pulmonary hypertension (gene PPH1) is caused by mutations in the bone morphogenetic protein receptor-II gene. *Am J Hum Genet* 2000, 67:737–744
6. Atkinson C, Stewart S, Upton PD, Machado R, Thomson JR, Trembath RC, Morrell NW: Primary pulmonary hypertension is associated with reduced pulmonary vascular expression of type II bone morphogenetic protein receptor. *Circulation* 2002, 105:1672–1678
7. Machado RD, Aldred MA, James V, Harrison RE, Patel B, Schwalbe EC, Gruenig E, Janssen B, Koehler R, Seeger W, Eickelberg O, Olschewski H, Elliott CG, Glissmeyer E, Carlquist J, Kim M, Torbicki A, Fijalkowska A, Szewczyk G, Parma J, Abramowicz MJ, Galie N, Morisaki H, Kyotani S, Nakanishi N, Morisaki T, Humbert M, Simonneau G, Sitbon O, Soubrier F, Coulet F, Morrell NW, Trembath RC: Mutations of the TGF-beta type II receptor BMPR2 in pulmonary arterial hypertension. *Hum Mutat* 2006, 27:121–132
8. Cogan JD, Pauciulo MW, Batchman AP, Prince MA, Robbins IM, Hedges LK, Stanton KC, Wheeler LA, Phillips III JA, Loyd JE, Nichols WC: High frequency of BMPR2 exonic deletions/duplications in familial pulmonary arterial hypertension. *Am J Respir Crit Care Med* 2006, 174:590–598
9. Thomson JR, Machado RD, Pauciulo MW, Morgan NV, Humbert M, Elliott GC, Ward K, Yacoub M, Mikhail G, Rogers P, Newman J, Wheeler L, Higenbottam T, Gibbs JS, Egan J, Crozier A, Peacock A, Allcock R, Corris P, Loyd JE, Trembath RC, Nichols WC: Sporadic primary pulmonary hypertension is associated with germline mutations of the gene encoding BMPR-II, a receptor member of the TGF-beta family. *J Med Genet* 2000, 37:741–745
10. Morisaki H, Nakanishi N, Kyotani S, Takashima A, Tomoike H, Morisaki T: BMPR2 mutations found in Japanese patients with familial and sporadic primary pulmonary hypertension. *Hum Mutat* 2004, 23:632
11. Aldred MA, Vijaykrishnan J, James V, Soubrier F, Gomez-Sanchez MA, Martensson G, Galie N, Manes A, Corris P, Simonneau G, Humbert M, Morrell NW, Trembath RC: BMPR2 gene rearrangements account for a significant proportion of mutations in familial and idiopathic pulmonary arterial hypertension. *Hum Mutat* 2006, 27:212–213
12. Koehler R, Grunig E, Pauciulo MW, Hoepfer MM, Olschewski H, Wilkens H, Halank M, Winkler J, Ewert R, Bremer H, Kreuzer S, Janssen B, Nichols WC: Low frequency of BMPR2 mutations in a German cohort of patients with sporadic idiopathic pulmonary arterial hypertension. *J Med Genet* 2004, 41:e127
13. Pepper MS: Transforming growth factor-beta: vasculogenesis, angiogenesis, and vessel wall integrity. *Cytokine Growth Factor Rev* 1997, 8:21–43
14. McCaffrey TA: TGF-betas and TGF-beta receptors in atherosclerosis. *Cytokine Growth Factor Rev* 2000, 11:103–114
15. Taraseviciene-Stewart L, Kasahara Y, Alger L, Hirth P, Mc Mahon G, Waltenberger J, Voelkel NF, Tuder RM: Inhibition of the VEGF receptor 2 combined with chronic hypoxia causes cell death-dependent pulmonary endothelial cell proliferation and severe pulmonary hypertension. *FASEB J* 2001, 15:427–438
16. Teichert-Kuliszewska K, Kutryk MJ, Kuliszewski MA, Karoubi G, Courtman DW, Zucco L, Granton J, Stewart DJ: Bone morphogenetic protein receptor-2 signaling promotes pulmonary arterial endothelial cell survival: implications for loss-of-function mutations in the pathogenesis of pulmonary hypertension. *Circ Res* 2006, 98:209–217
17. Masri FA, Xu W, Comhair SA, Asosingh K, Koo M, Vasanji A, Drazba J, Anand-Apte B, Erzurum SC: Hyperproliferative apoptosis-resistant endothelial cells in idiopathic pulmonary arterial hypertension. *Am J Physiol* 2007, 293:L548–L554
18. Phillips RJ, Burdick MD, Hong K, Lutz MA, Murray LA, Xue YY, Belperio JA, Keane MP, Strieter RM: Circulating fibrocytes traffic to the lungs in response to CXCL12 and mediate fibrosis. *J Clin Invest* 2004, 114:438–446
19. Frid MG, Brunetti JA, Burke DL, Carpenter TC, Davie NJ, Reeves JT, Roederseimer MT, van Rooijen N, Stenmark KR: Hypoxia-induced pulmonary vascular remodeling requires recruitment of circulating mesenchymal precursors of a monocyte/macrophage lineage. *Am J Pathol* 2006, 168:659–669
20. Asosingh K, Swaidani S, Aronica M, Erzurum SC: Th1- and Th2-dependent endothelial progenitor cell recruitment and angiogenic switch in asthma. *J Immunol* 2007, 178:6482–6494
21. Strieter RM, Gomperts BN, Keane MP: The role of CXC chemokines in pulmonary fibrosis. *J Clin Invest* 2007, 117:549–556
22. Stenmark KR, Fagan KA, Frid MG: Hypoxia-induced pulmonary vascular remodeling: cellular and molecular mechanisms. *Circ Res* 2006, 99:675–691
23. Hur J, Yang HM, Yoon CH, Lee CS, Park KW, Kim JH, Kim TY, Kim JY, Kang HJ, Chae IH, Oh BH, Park YB, Kim HS: Identification of a novel role of T cells in postnatal vasculogenesis: characterization of endothelial progenitor cell colonies. *Circulation* 2007, 116:1671–1682
24. Asahara T, Murohara T, Sullivan A, Silver M, van der Zee R, Li T, Witzenbichler B, Schatteman G, Isner JM: Isolation of putative progenitor endothelial cells for angiogenesis. *Science* 1997, 275:964–967
25. Pesce M, Orlandi A, Iachininoto MG, Straino S, Torella AR, Rizzuti V, Pompilio G, Bonanno G, Scambia G, Capogrossi MC: Myoendothelial differentiation of human umbilical cord blood-derived stem cells in ischemic limb tissues. *Circ Res* 2003, 93:e51–e62
26. Gehling UM, Ergun S, Schumacher U, Wagener C, Pantel K, Otte M, Schuch G, Schafhausen P, Mende T, Kilic N, Kluge K, Schafer B, Hossfeld DK, Fiedler W: In vitro differentiation of endothelial cells from AC133-positive progenitor cells. *Blood* 2000, 95:3106–3112
27. Prater DN, Case J, Ingram DA, Yoder MC: Working hypothesis to redefine endothelial progenitor cells. *Leukemia* 2007, 21:1141–1149
28. Rehman J, Li J, Orschell CM, March KL: Peripheral blood “endothelial progenitor cells” are derived from monocyte/macrophages and secrete angiogenic growth factors. *Circulation* 2003, 107:1164–1169
29. Zhang SJ, Zhang H, Wei YJ, Su WJ, Liao ZK, Hou M, Zhou JY, Hu SS: Adult endothelial progenitor cells from human peripheral blood maintain monocyte/macrophage function throughout in vitro culture. *Cell Res* 2006, 16:577–584
30. Kalka C, Masuda H, Takahashi T, Kalka-Moll WM, Silver M, Kearney M, Li T, Isner JM, Asahara T: Transplantation of ex vivo expanded endothelial progenitor cells for therapeutic neovascularization. *Proc Natl Acad Sci USA* 2000, 97:3422–3427
31. Kawamoto A, Gwon HC, Iwaguro H, Yamaguchi JI, Uchida S, Masuda H, Silver M, Ma H, Kearney M, Isner JM, Asahara T: Therapeutic potential of ex vivo expanded endothelial progenitor cells for myocardial ischemia. *Circulation* 2001, 103:634–637
32. Rehman J, Li J, Parvathaneni L, Karlsson G, Panchal VR, Temm CJ, Mahenthiran J, March KL: Exercise acutely increases circulating endothelial progenitor cells and monocyte/macrophage-derived angiogenic cells. *J Am Coll Cardiol* 2004, 43:2314–2318
33. Hill JM, Zalos G, Halcox JP, Schenke WH, Waclawiw MA, Quyyumi AA, Finkel T: Circulating endothelial progenitor cells, vascular function, and cardiovascular risk. *N Engl J Med* 2003, 348:593–600
34. Loomans CJ, de Koning EJ, Staal FJ, Rookmaaker MB, Verseyden C, de Boer HC, Verhaar MC, Braam B, Rabelink TJ, van Zonneveld AJ: Endothelial progenitor cell dysfunction: a novel concept in the pathogenesis of vascular complications of type 1 diabetes. *Diabetes* 2004, 53:195–199
35. Palange P, Testa U, Huertas A, Calabro L, Antonucci R, Petrucci E,

- Pelosi E, Pasquini L, Satta A, Morici G, Vignola MA, Bonsignore MR: Circulating haemopoietic and endothelial progenitor cells are decreased in COPD. *Eur Respir J* 2006, 27:529–541
36. Valgimigli M, Rigolin GM, Fucili A, Porta MD, Soukhomovskaia O, Malagutti P, Bugli AM, Bragotti LZ, Francolini G, Mauro E, Castoldi G, Ferrari R: CD34+ and endothelial progenitor cells in patients with various degrees of congestive heart failure. *Circulation* 2004, 110:1209–1212
  37. Grisar J, Aletaha D, Steiner CW, Kapral T, Steiner S, Seidinger D, Weigel G, Schwarzwinger I, Wolozczuk W, Steiner G, Smolen JS: Depletion of endothelial progenitor cells in the peripheral blood of patients with rheumatoid arthritis. *Circulation* 2005, 111:204–211
  38. Hur J, Yoon CH, Kim HS, Choi JH, Kang HJ, Hwang KK, Oh BH, Lee MM, Park YB: Characterization of two types of endothelial progenitor cells and their different contributions to neovasculogenesis. *Arterioscler Thromb Vasc Biol* 2004, 24:288–293
  39. Shepherd RM, Capoccia BJ, Devine SM, Dipersio J, Trinkaus KM, Ingram D, Link DC: Angiogenic cells can be rapidly mobilized and efficiently harvested from the blood following treatment with AMD3100. *Blood* 2006, 108:3662–3667
  40. Güven H, Shepherd RM, Bach RG, Capoccia BJ, Link DC: The number of endothelial progenitor cell colonies in the blood is increased in patients with angiographically significant coronary artery disease. *J Am Coll Cardiol* 2006, 48:1579–1587
  41. Ingram DA, Mead LE, Tanaka H, Meade V, Fenoglio A, Mortell K, Pollok K, Ferkowicz MJ, Gilley D, Yoder MC: Identification of a novel hierarchy of endothelial progenitor cells using human peripheral and umbilical cord blood. *Blood* 2004, 104:2752–2760
  42. Amos-Landgraf JM, Cottle A, Plenge RM, Friez M, Schwartz CE, Longshore J, Willard HF: X chromosome-inactivation patterns of 1,005 phenotypically unaffected females. *Am J Hum Genet* 2006, 79:493–499
  43. Murasawa S, Asahara T: Endothelial progenitor cells for vasculogenesis. *Physiology (Bethesda)* 2005, 20:36–42
  44. Urbich C, Dimmeler S: Endothelial progenitor cells: characterization and role in vascular biology. *Circ Res* 2004, 95:343–353
  45. Crosby JR, Kaminski WE, Schatteman G, Martin PJ, Raines EW, Seifert RA, Bowen-Pope DF: Endothelial cells of hematopoietic origin make a significant contribution to adult blood vessel formation. *Circ Res* 2000, 87:728–730
  46. Morrell NW, Yang X, Upton PD, Jourdan KB, Morgan N, Sheares KK, Trembath RC: Altered growth responses of pulmonary artery smooth muscle cells from patients with primary pulmonary hypertension to transforming growth factor-beta(1) and bone morphogenetic proteins. *Circulation* 2001, 104:790–795
  47. Smith P, Heath D: Electron microscopy of the plexiform lesion. *Thorax* 1979, 34:177–186
  48. Tudor RM, Groves B, Badesch DB, Voelkel NF: Exuberant endothelial cell growth and elements of inflammation are present in plexiform lesions of pulmonary hypertension. *Am J Pathol* 1994, 144:275–285
  49. Dorfmueller P, Perros F, Balabanian K, Humbert M: Inflammation in pulmonary arterial hypertension. *Eur Respir J* 2003, 22:358–363
  50. Stabile E, Burnett MS, Watkins C, Kinnaird T, Bachis A, la Sala A, Miller JM, Shou M, Epstein SE, Fuchs S: Impaired arteriogenic response to acute hindlimb ischemia in CD4-knockout mice. *Circulation* 2003, 108:205–210
  51. Stabile E, Kinnaird T, la Sala A, Hanson SK, Watkins C, Campia U, Shou M, Zbinden S, Fuchs S, Kornfeld H, Epstein SE, Burnett MS: CD8+ T lymphocytes regulate the arteriogenic response to ischemia by infiltrating the site of collateral vessel development and recruiting CD4+ mononuclear cells through the expression of interleukin-16. *Circulation* 2006, 113:118–124
  52. Urbich C, Aicher A, Heeschen C, Dernbach E, Hofmann WK, Zeiher AM, Dimmeler S: Soluble factors released by endothelial progenitor cells promote migration of endothelial cells and cardiac resident progenitor cells. *J Mol Cell Cardiol* 2005, 39:733–742
  53. Cheng XW, Kuzuya M, Nakamura K, Maeda K, Tsuzuki M, Kim W, Sasaki T, Liu Z, Inoue N, Kondo T, Jin H, Numaguchi Y, Okumura K, Yokota M, Iguchi A, Murohara T: Mechanisms underlying the impairment of ischemia-induced neovascularization in matrix metalloproteinase 2-deficient mice. *Circ Res* 2007, 100:904–913
  54. Jin DK, Shido K, Kopp HG, Petit I, Shmelkov SV, Young LM, Hooper AT, Amano H, Avecilla ST, Heissig B, Hattori K, Zhang F, Hicklin DJ, Wu Y, Zhu Z, Dunn A, Salari H, Werb Z, Hackett NR, Crystal RG, Lyden D, Rafii S: Cytokine-mediated deployment of SDF-1 induces revascularization through recruitment of CXCR4+ hemangiocytes. *Nat Med* 2006, 12:557–567
  55. Kuzuya M, Kanda S, Sasaki T, Tamaya-Mori N, Cheng XW, Itoh T, Itohara S, Iguchi A: Deficiency of gelatinase suppresses smooth muscle cell invasion and development of experimental intimal hyperplasia. *Circulation* 2003, 108:1375–1381
  56. Zhang S, Zhang D, Sun B: Vasculogenic mimicry: current status and future prospects. *Cancer Lett* 2007, 254:156–164
  57. Ceradini DJ, Kulkarni AR, Callaghan MJ, Tepper OM, Bastidas N, Kleinman ME, Capla JM, Galiano RD, Levine JP, Gurtner GC: Progenitor cell trafficking is regulated by hypoxic gradients through HIF-1 induction of SDF-1. *Nat Med* 2004, 10:858–864
  58. Hayashida K, Fujita J, Miyake Y, Kawada H, Ando K, Ogawa S, Fukuda K: Bone marrow-derived cells contribute to pulmonary vascular remodeling in hypoxia-induced pulmonary hypertension. *Chest* 2005, 127:1793–1798
  59. Davie NJ, Crossno JT Jr, Frid MG, Hofmeister SE, Reeves JT, Hyde DM, Carpenter TC, Brunetti JA, McNiece IK, Stenmark KR: Hypoxia-induced pulmonary artery adventitial remodeling and neovascularization: contribution of progenitor cells. *Am J Physiol* 2004, 286:L668–L678
  60. Dingli D, Utz JP, Krowka MJ, Oberg AL, Tefferi A: Unexplained pulmonary hypertension in chronic myeloproliferative disorders. *Chest* 2001, 120:801–808
  61. Garypidou V, Vakalopoulou S, Dimitriadis D, Tziomalos K, Sfikas G, Perifanis V: Incidence of pulmonary hypertension in patients with chronic myeloproliferative disorders. *Haematologica* 2004, 89:245–246
  62. Hoffman R, Xu M: Is bone marrow fibrosis the real problem? *Blood* 2006, 107:3421–3422
  63. Rossoff LJ, Genovese J, Coleman M, Dantzker DR: Primary pulmonary hypertension in a patient with CD8/T-cell large granulocyte leukemia: amelioration by cladribine therapy. *Chest* 1997, 112:551–553
  64. Steensma DP, Hook CC, Stafford SL, Tefferi A: Low-dose, single-fraction, whole-lung radiotherapy for pulmonary hypertension associated with myelofibrosis with myeloid metaplasia. *Br J Haematol* 2002, 118:813–816
  65. Zhao YD, Courtman DW, Deng Y, Kugathasan L, Zhang Q, Stewart DJ: Rescue of monocrotaline-induced pulmonary arterial hypertension using bone marrow-derived endothelial-like progenitor cells: efficacy of combined cell and eNOS gene therapy in established disease. *Circ Res* 2005, 96:442–450